Journal of Computational Physics 508 (2024) 113036

Contents lists available at ScienceDirect

Journal of Computational Physics

journal homepage: www.elsevier.com/locate/jcp

Weak solutions for extended magnetohydrodynamics using linear combination of entropies

Gábor Tóth *, Bart van der Holst

University of Michigan, 2455 Hayward St, Ann Arbor, MI, 48109, USA

ARTICLE INFO

Keywords:
Weak solution
Conservation laws
Extended magnetohydrodynamics

ABSTRACT

It is commonplace to solve the extended magnetohydrodynamics (MHD) system of equations in non-conservative form, in particular using equations for pressures. This approach leads to unpredictable behavior at discontinuities such as shock fronts. Here we propose using a linear combination of entropy densities to distribute the non-adiabatic heating among the various pressure components in a deterministic manner. In particular, we describe algorithms that can distribute the non-adiabatic heating between electrons and ions when the electron and ion temperatures are solved separately, and between parallel and perpendicular pressures for anisotropic pressure MHD. The same approach can also be used for extended hydrodynamic equations. The algorithm is based on conservation laws, which provides proper convergence to weak solutions as demonstrated by numerical tests.

1. Introduction

The ideal magnetohydrodynamic (MHD) equations can be written in a conservation form in terms of mass, momentum and energy densities and magnetic field. A conservative discretization of these equations guarantees correct weak solutions across discontinuities, in particular across MHD shocks. When ideal MHD is extended to account for pressure anisotropy and/or electron pressure being different from ion pressure [1–3], there is no obvious way to write the extended MHD equations in a conservative form that is correct across discontinuities, such as shocks and current sheets. In reality, the distribution of the total energy density among electron, ion and/or parallel and perpendicular energy densities is determined by physical processes at the shock front or the current sheet that are not captured by the extended MHD equations, which represents them as discontinuities. This means that the electrons pressure downstream the bow shock of Earth or the ratio of parallel and perpendicular ion pressures behind a shock produced by a coronal mass ejection are not realistic in the simulation and may not even converge to a deterministic value with increasing grid resolution.

Here we propose an algorithm to handle both ion pressure anisotropy and separate electron pressure in a way that provides weak solutions that are similar to shocks observed in space by satellites or simulated with kinetic models. In particular, we propose to solve for the total energy density (in conservation form), together with linear combinations of entropy densities (instead of pressures). The entropy equations are in conservation form for electrons [4] as well as for the parallel and perpendicular ion entropy densities [5]. The weights in the linear combinations can be used to determine how the non-adiabatic processes increase the individual entropy densities and corresponding pressures. The conservation form guarantees that the solution is well-behaved across discontinuities, which is not true for the non-conservative pressure equations.

* Corresponding author.
E-mail address: gtoth@umich.edu (G. Tóth).

https://doi.org/10.1016/j.jcp.2024.113036
Received 14 September 2023; Received in revised form 1 April 2024; Accepted 17 April 2024

Available online 22 April 2024

In general, the non-adiabatic heating fractions are not constants. Electron heating across shocks has been studied with kinetic simulations, and it was found that a non-zero fraction W_e of the total non-adiabatic heating is deposited into the electron energy density [6]. For the anisotropic ion pressure, let us consider the two extreme cases: parallel shocks where the magnetic field $\mathbf{B}$ is parallel with the shock normal $\mathbf{n}$, and perpendicular shocks with $\mathbf{B}\cdot\mathbf{n}=0$. We expect that for parallel shocks most of the non-adiabatic heating is deposited into the parallel entropy, while for perpendicular shocks most of the non-adiabatic heating goes into the perpendicular entropy. We note that the anisotropy may be limited by instabilities [2]. Our algorithm accommodates non-constant weights as long as the variation of the weights is smooth across the discontinuities.

Section 2 describes the extended MHD equations in various forms, including the entropy and pressure equations. Section 3 describes the new algorithm. Numerical tests are presented in Section 4, and we conclude in Section 5.

2. Extended MHD equations using entropy

The extended MHD equations in a conservative form [1,2] can be written as

$$\frac{\partial \rho}{\partial t} + \nabla\cdot(\rho\mathbf{u}) = S_\rho \tag{1}$$

$$\frac{\partial \rho\mathbf{u}}{\partial t} + \nabla\cdot\left(\rho\mathbf{u}\mathbf{u} - \mathbf{B}\mathbf{B} + (p_\parallel - p_\perp)\mathbf{b}\mathbf{b} + I\,p + I\,\frac{B^2}{2}\right) = \mathbf{S}_{\rho\mathbf{u}} \tag{2}$$

$$\frac{\partial e}{\partial t} + \nabla\cdot\left(e\mathbf{u} + p\mathbf{u} + \frac{B^2}{2}\mathbf{u} - \mathbf{B}\mathbf{B}\cdot\mathbf{u} + (p_\parallel - p_\perp)\mathbf{b}\mathbf{b}\cdot\mathbf{u}\right) = S_e \tag{3}$$

$$\frac{\partial \mathbf{B}}{\partial t} + \nabla\times(-\mathbf{u}\times\mathbf{B}) = \mathbf{S}_\mathbf{B} \tag{4}$$

where ρ is the mass density, $\mathbf{u}$ is the bulk velocity, $\mathbf{B}$ the magnetic field vector, $\mathbf{b}=\mathbf{B}/B$ is the unit vector parallel with $\mathbf{B}$ and $p=p_\perp+p_e$. The magnetic field units are chosen to make the magnetic permeability $\mu_0=1$. The isotropic ion pressure equations can be obtained by setting $p_\parallel=p_\perp=p_i$. Setting $p_e=0$ eliminates the separate electron pressure. Finally, setting $\mathbf{B}=0$ results in the hydrodynamic equations. The source terms on the right hand sides are zero for ideal MHD, but they may differ from zero in general. The total energy density is

$$e = \frac{\rho u^2}{2} + \frac{B^2}{2} + e_t = \frac{\rho u^2}{2} + \frac{B^2}{2} + e_i + e_e \tag{5}$$

where e_t is the total thermal energy density, $e_i=e_\parallel+e_\perp$ is the ion thermal energy density, and e_e is the electron thermal energy density. The energy densities are related to the pressures as

$$e_\alpha = \frac{p_\alpha}{\gamma_\alpha - 1} \tag{6}$$

where α stands for $e, i, \parallel$ or $\perp$. The adiabatic indexes are $\gamma_i=5/3$, $\gamma_\parallel=3$ and $\gamma_\perp=2$ from the $\gamma=(F+2)/F$ relationship with F the degrees of freedom. The electron adiabatic index γ_e can be different from γ_i in general.

The specific entropy density (per unit mass) of a gas is usually defined as $\sigma=\ln(Cp/\rho^\gamma)$ from the Sackur–Tetrode equation where C is some constant with appropriate dimensions. One can define the volumetric entropy density as $s=\rho f(\sigma)$, where f is an arbitrary differentiable function (see Appendix A and Appendix B). We can choose $f(\sigma)=\exp(\sigma)/C$ so that $s=p/\rho^{\gamma-1}$ is a linear function of pressure p. Analogously, the volumetric electron entropy density can be defined as

$$s_e = \frac{\gamma_e - 1}{\rho^{\gamma_e-1}} e_e \tag{7}$$

where we used Eq. (6) to express p_e from e_e. If the ion pressure is assumed to be isotropic, the ion entropy density is

$$s_i = \frac{\gamma_i - 1}{\rho^{\gamma_i-1}} e_i \tag{8}$$

In the anisotropic ion pressure case [5], the parallel and perpendicular ion entropy densities (see also Appendix A) that are linear functions of the energy densities are

$$s_\parallel = \frac{2B^2}{\rho^2} e_\parallel \tag{9}$$

$$s_\perp = \frac{1}{B} e_\perp \tag{10}$$

All entropy densities satisfy a simple conservation law (for smooth solutions):

$$\frac{\partial s_\alpha}{\partial t} + \nabla\cdot(s_\alpha\mathbf{u}) = S_{s_\alpha} \tag{11}$$

Using different functions f_α to define $s'_\alpha=\rho f_\alpha(s_\alpha/\rho)$ lead to alternative definitions of entropy densities that all satisfy the conservation law (11). The particular choices above have linear dependence on energy densities, $s_\alpha \propto e_\alpha$, which will be useful later

on. Combining these conservation laws with the definitions of the entropy densities leads to the usual non-conservative pressure equations (see Appendix A). The electron pressure equation:

$$\frac{\partial p_e}{\partial t} + \nabla \cdot (p_e \mathbf{u}) + (\gamma_e - 1) p_e \nabla \cdot \mathbf{u} = S_{p_e} \tag{12}$$

For isotropic ion pressure the ion pressure equation:

$$\frac{\partial p_i}{\partial t} + \nabla \cdot (p_i \mathbf{u}) + (\gamma_i - 1) p_i \nabla \cdot \mathbf{u} = S_{p_i} \tag{13}$$

For anisotropic ion pressure the parallel and perpendicular pressure equations:

$$\frac{\partial p_\parallel}{\partial t} + \nabla \cdot (p_\parallel \mathbf{u}) + 2 p_\parallel \mathbf{b} \cdot (\mathbf{b} \cdot \nabla) \mathbf{u} = S_{p_\parallel} \tag{14}$$

$$\frac{\partial p_\perp}{\partial t} + \nabla \cdot (p_\perp \mathbf{u}) + p_\perp \nabla \cdot \mathbf{u} - p_\perp \mathbf{b} \cdot (\mathbf{b} \cdot \nabla) \mathbf{u} = S_{p_\perp} \tag{15}$$

The entropy source terms are obtained by taking the time derivatives of Eqs. (7)–(10) (see Appendix A for a detailed derivation):

$$S_{s_e} = \frac{1}{\rho^{\gamma_e - 1}} S_{p_e} - (\gamma_e - 1) \frac{p_e}{\rho^{\gamma_e}} S_\rho \tag{16}$$

$$S_{s_i} = \frac{1}{\rho^{\gamma_i - 1}} S_{p_i} - (\gamma_i - 1) \frac{p_i}{\rho^{\gamma_i}} S_\rho \tag{17}$$

$$S_{s_\parallel} = \frac{B^2}{\rho^2} S_{p_\parallel} + 2 \frac{p_\parallel}{\rho^2} \mathbf{B} \cdot \mathbf{S}'_{\mathbf{B}} - 2 \frac{p_\parallel B^2}{\rho^3} S_\rho \tag{18}$$

$$S_{s_\perp} = \frac{1}{B} S_{p_\perp} - \frac{p_\perp}{B^3} \mathbf{B} \cdot \mathbf{S}'_{\mathbf{B}} \tag{19}$$

where $\mathbf{S}'_{\mathbf{B}} = \mathbf{S}_{\mathbf{B}} + \mathbf{u} \nabla \cdot \mathbf{B}$, i.e. if the 8-wave [7] source term $-\mathbf{u} \nabla \cdot \mathbf{B}$ is used in the induction equation, then it does not enter the entropy source terms $S_{s_\parallel}$ and $S_{s_\perp}$.

3. Distributing the non-adiabatic heating

Solving the conservative energy equation (3) provides a time derivative, or in the discrete sense a change, for the energy density, which we denote as Δe. Solving the discrete form of the entropy density equations (11) provides preliminary updates for s_α, and the corresponding thermal energy densities e_α from Eq. (7)–(10). We denote this preliminary (adiabatic) change as $\Delta_s e_\alpha$ where the s subscript indicates that the update is based on an entropy conservation law. The update of the thermal energy e_t based on the total energy equation (3) and Eq. (5) and the adiabatic updates of energy densities e_α based on Eq. (11) are related as

$$\Delta e_t = \Delta_s e_e + \Delta_s e_i + \Delta e_n \tag{20}$$

where the last term $\Delta e_n \equiv \Delta e_t - \Delta_s e_e - \Delta_s e_i$ describes the non-adiabatic heating. For well-resolved smooth solutions $\Delta e_n = 0$ within truncation error. Across a discontinuity, however, $\Delta e_n \neq 0$. In the anisotropic case the adiabatic change in the ion thermal energy consists of the sum of the parallel and perpendicular adiabatic energy changes:

$$\Delta_s e_i = \Delta_s e_\parallel + \Delta_s e_\perp \tag{21}$$

3.1. Distributing non-adiabatic heating between isotropic electron and ion pressures

First we discuss the distribution of the non-adiabatic energy between electrons and ions with an isotropic ion pressure. Assuming that a fraction W_i of this energy goes into the ions and $W_e = 1 - W_i$ into the electrons, we can define the ion and electron thermal energy updates as

$$\Delta e_i = \Delta_s e_i + W_i \Delta e_n \tag{22}$$

$$\Delta e_e = \Delta_s e_e + W_e \Delta e_n \tag{23}$$

Setting $W_e = 0$ assumes that the electrons are heated adiabatically, which is not valid based on kinetic simulations [6] and satellite observations [8] that suggest $W_e \approx 1/4$.

It is not entirely obvious that the updates Eqs. (22) and (23), which can be viewed as adding and subtracting source terms, will not have the same issue as solving the non-conservative pressure equations: the solution may depend on the discretization errors at the shock front. There is a good reason to believe that is not the case as long as $\gamma_i = \gamma_e$. In this particular case moving energy between e_i and e_e will not change the total pressure $p = p_i + p_e$, which is the only form of pressure entering the momentum equation (2), energy equation (3) and the definition of the energy density Eq. (5).

When $\gamma_i \neq \gamma_e$, we have to specify the shock heating of electrons and ions in a manner that relies on conservation laws. We introduce a “combined entropy” density

$$s_{ie} = W_e s_i - W_i s_e \tag{24}$$

that needs to be conserved. The non-negative weights satisfy $W_i + W_e = 1$ (although this is not essential). We take the difference instead of the sum, as we expect the non-adiabatic heating to increase both the ion and electron entropy densities, so it is their weighted difference that can be conserved. Clearly, s_{ie} satisfies a conservation law similar to s_α in Eq. (11). If $W_e = 1$ then the ion entropy is conserved, so all non-adiabatic heating is pushed into the electrons. If $W_e = 0$, then the electron entropy is conserved (since $s_{ie} = -s_e$ is conserved), and all non-adiabatic heating is deposited into the ions. In the general case, one needs to solve the following two equations for the unknowns e_i and e_e:

$$w_e e_i - w_i e_e = s_{ie} \tag{25}$$

$$e_i + e_e = e_t \tag{26}$$

where we introduced the energy weights $w_e = W_e(\gamma_i - 1)/\rho^{\gamma_i - 1}$ and $w_i = W_i(\gamma_e - 1)/\rho^{\gamma_e - 1}$ based on Eqs. (7) and (8). The solutions are

$$\begin{aligned} e_i &= \frac{s_{ie} + w_i e_t}{w_e + w_i} \\ e_e &= e_t - e_i \end{aligned} \tag{27}$$

With some manipulations, the equations can be rewritten into an update form:

$$\begin{aligned} \Delta e_i &= \Delta_s e_i + \frac{w_i}{w_i + w_e}\Delta e_n = \Delta_s e_i + \frac{W_i}{W_i + W_e \frac{\rho^{\gamma_e}}{\rho^{\gamma_i}} \frac{\gamma_i - 1}{\gamma_e - 1}}\Delta e_n \\ \Delta e_e &= \Delta_s e_e + \frac{w_e}{w_e + w_i}\Delta e_n = \Delta_s e_e + \frac{W_e}{W_e + W_i \frac{\rho^{\gamma_i}}{\rho^{\gamma_e}} \frac{\gamma_e - 1}{\gamma_i - 1}}\Delta e_n \end{aligned} \tag{28}$$

For the case $\gamma_e = \gamma_i$, these equations become the same as Eqs. (22) and (23), which confirms that Eqs. (22) and (23) will produce correct weak solutions for this case.

The weights W_e and W_i can vary smoothly and slowly across the shock, and the solution will remain well-behaved. For example, the weights can depend on the plasma beta or the Mach number upstream of the shock front.

3.2. Distributing non-adiabatic heating between parallel and perpendicular ion pressures

In the anisotropic ion pressure case (starting with no electron pressure equation here, and continuing with electron pressure in subsection 3.3), the goal is to distribute the non-adiabatic energy gain Δe_n between the parallel and perpendicular thermal energies $e_\parallel$ and $e_\perp$. Using weights $W_\perp$ and $W_\parallel = 1 - W_\perp$, the combined entropy to be conserved is defined as

$$s_\times = W_\perp s_\parallel - W_\parallel s_\perp \tag{29}$$

which satisfies the same conservation law as $s_\perp$ and $s_\parallel$. When $W_\perp = 1$, the parallel entropy is conserved, so all non-adiabatic heating is pushed into the perpendicular pressure. Conversely, when $W_\perp = 0$, all non-adiabatic heating is deposited into the parallel pressure.

In the general case, the following system of equations need to be solved for $e_\parallel$ and $e_\perp$:

$$w_\perp e_\parallel - w_\parallel e_\perp = s_\times \tag{30}$$

$$e_\parallel + e_\perp = e_t \tag{31}$$

where we introduced the energy weights $w_\perp = W_\perp 2B^2/\rho^2$ and $w_\parallel = W_\parallel/B$. The solutions are

$$\begin{aligned} e_\parallel &= \frac{s_\times + w_\parallel e_t}{w_\perp + w_\parallel} \\ e_\perp &= e_t - e_\parallel \end{aligned} \tag{32}$$

After some simple algebra, the equations can be written into an update form

$$\begin{aligned} \Delta e_\parallel &= \Delta_s e_\parallel + \frac{w_\parallel}{w_\parallel + w_\perp}\Delta e_n = \Delta_s e_\parallel + \frac{W_\parallel}{W_\parallel + W_\perp 2B^3/\rho^2}\Delta e_n \\ \Delta e_\perp &= \Delta_s e_\perp + \frac{w_\perp}{w_\perp + w_\parallel}\Delta e_n = \Delta_s e_\perp + \frac{W_\perp}{W_\perp + W_\parallel \rho^2/(2B^3)}\Delta e_n \end{aligned} \tag{33}$$

For $W_\parallel = 0$ the $\Delta e_\parallel$ update is purely adiabatic and all non-adiabatic heating is deposited into $\Delta e_\perp$, while for $W_\perp = 0$ the opposite holds. For $0 < W_\parallel < 1$ a fraction of the shock heating is deposited into $e_\parallel$, but this fraction depends on B^3/ρ^2, which is the ratio of the coefficients of the parallel and perpendicular entropy densities in Eqs. (9) and (10).

The weights $W_\parallel$ and $W_\perp = 1 - W_\parallel$ do not have to be global constants. As long as they change smoothly and slowly across the shock, the solution will remain well-behaved. For example, one can make $W_\parallel$ a function of the upstream angle θ_1 between the magnetic field $\mathbf{B}_1$ and the shock normal $\mathbf{n}$ directions:

$$W_\parallel = \cos\theta_1 = \frac{|\mathbf{n}\cdot\mathbf{B}_1|}{B_1} \tag{34}$$

where the subscript 1 refers to the upstream values. With this definition, $W_\parallel = 1$ and 0 for parallel and perpendicular shocks, respectively. For a moving shock, the shock normal direction can be obtained from the change of velocity $\Delta\mathbf{u}$, for example.

3.3. Distributing non-adiabatic heating among electron, parallel and perpendicular pressures

Finally, we discuss the most complicated case, when we solve for the isotropic electron pressure and anisotropic ion pressures (parallel and perpendicular). We define two linear combinations of the entropy densities:

$$s_{ie} = W_e s_\parallel - W_i s_e \tag{35}$$

$$s_\times = W_\perp s_\parallel - W_\parallel s_\perp \tag{36}$$

where W_e and W_i define how the non-adiabatic heating increases the electron and parallel ion entropy densities. The choice of $s_\parallel$ over $s_\perp$ is arbitrary. Unfortunately using the sum of the two ion entropy densities is not particularly better, as they have different physical dimensions. Similarly, $W_\parallel$ and $W_\perp$ determines the split between $s_\parallel$ and $s_\perp$. The weights are positive and satisfy $W_i + W_e = 1$ and $W_\parallel + W_\perp = 1$. After updating the total energy and the entropy densities, we solve the following linear system of equations for e_e, $e_\parallel$ and $e_\perp$:

$$w_e e_\parallel - w_i e_e = s_{ie} \tag{37}$$

$$w_\perp e_\parallel - w_\parallel e_\perp = s_\times \tag{38}$$

$$e_e + e_\parallel + e_\perp = e_t \tag{39}$$

where the energy weights are $w_i = W_i(\gamma_e - 1)/\rho^{\gamma_e - 1}$, $w_e = W_e B^2/\rho^2$, $w_\parallel = W_\parallel/B$ and $w_\perp = W_\perp 2B^2/\rho^2$. The solutions are

$$\begin{aligned} e_\parallel &= \frac{w_\parallel s_{ie} + w_i s_\times + w_i w_\parallel e_t}{w_\perp w_i + w_\parallel w_e + w_i w_\parallel} \\ e_\perp &= \frac{w_\perp e_\parallel - s_\times}{w_\parallel} \\ e_e &= \frac{w_e e_\parallel - s_{ie}}{w_i} \end{aligned} \tag{40}$$

The coefficients $W_i = 1 - W_e$ and $W_\parallel = 1 - W_\perp$ can be smoothly varying functions.

3.4. Summary of the numerical scheme

Here we summarize the implementation of the numerical scheme. First we solve equations (1) to (4) for mass density ρ, momentum density $\rho\mathbf{u}$, total energy density e, magnetic field $\mathbf{B}$ and also the entropy conservation laws (11) for all entropy densities s_α. Next, we calculate the total thermal energy density e_t from Eq. (5) and the linear combinations of the entropy densities s_{ie} and/or $s_\times$ from Eqs. (24) or (35) and/or (29). Finally, we obtain the energy densities e_α from Eqs. (27), (32) or (40), and calculate the corresponding pressures p_α from Eq. (6).

4. Numerical tests

The schemes described above have been implemented into the BATS-R-US extended MHD code [9,10,1]. We will use normalized units throughout, so that $\mu_0 = k_B = M_i = 1$. The adiabatic indexes are 5/3 unless noted otherwise. Note that in all tests we solve Eq. (3) for the total energy density e defined by Eq. (5), so the total energy is always conserved. The new scheme differs from the other tested schemes in how the total energy density is distributed among the individual energy densities e_α.

4.1. 1D shocktube tests

We solve the anisotropic MHD equations with separate electron pressure on a 1D domain $-128 < x < 128$ resolved by 1500 grid cells, which is more than sufficient to obtain a grid converged solution (if the scheme solves conservation laws). The second order Rusanov [11] scheme is used with the minmod limiter applied to the primitive variables. The adiabatic index of the electrons is $\gamma_e = 5/3$. The stability conditions [12] for the anisotropy are not enforced, so the results of the scheme can be clearly understood. For the new scheme we use $W_e = 0.4$ (instead of 0.25) to make the electron pressure variation more obvious. The anisotropic weights

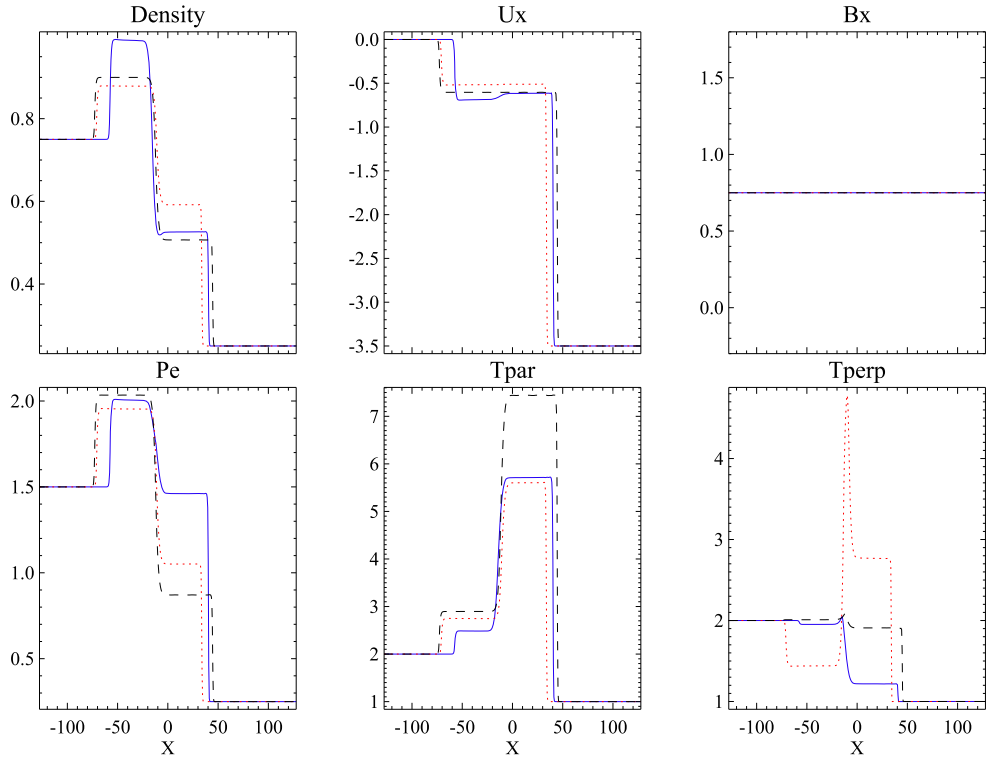

Fig. 1. Solution of the 1D parallel shock problem with the new algorithm solving for energy and entropy densities e, $s_{ie} = 0.4s_i - 0.6s_e$ and $s_\times = 0.1s_\parallel - 0.9s_\perp$ (solid blue line), with the conservative scheme solving for e, s_e and $s_\parallel$ (dotted red line), and with energy conserving MHD scheme extended with non-conservative pressure equations solving for e, p_e and $p_\parallel$ (dashed black line). (For interpretation of the colors in the figure(s), the reader is referred to the web version of this article.)

are set by Eq. (34) but limited to stay within $0.1 \le W_\parallel, W_\perp \le 0.9$. The initial conditions are piece-wise constant separated by a discontinuity at $x = 0$. The simulations are run to $t = 20$.

For the parallel shock the upstream state at $x > 0$ is $\rho_1 = 0.25$, $\mathbf{u}_1 = (-3.5, 0, 0)$, $\mathbf{B}_1 = (0.75, 0, 0)$, and $p_{e,1} = p_{\parallel,1} = p_{\perp,1} = 0.25$, while the downstream state at $x < 0$ is $\rho_2 = 0.75$, $\mathbf{u}_2 = 0$, $\mathbf{B}_2 = (0.75, 0, 0)$ and $p_{e,2} = p_{\parallel,2} = p_{\perp,2} = 1.5$. Fig. 1 shows the solutions obtained with our new scheme and the typical energy conserving MHD scheme combined with pressure or entropy equations. For the new scheme $W_\parallel = 0.9$, consequently the perpendicular temperature $T_\perp = p_\perp/\rho$ does not change much across the shock at $x \approx 50$, while the other schemes mostly deposit the shock heating into the perpendicular pressure and produce a larger jump in $T_\perp$.

For the perpendicular shock the upstream state at $x < 0$ is $\rho_1 = 0.25$, $\mathbf{u}_1 = (-3.5, 0, 0)$, $\mathbf{B}_1 = (0, 0.25, 0)$ and $p_{e,1} = p_{\parallel,1} = p_{\perp,1} = 0.25$, while the initial downstream state at $x > 0$ is $\rho_2 = 0.75$, $\mathbf{u}_2 = 0$, $\mathbf{B}_2 = (0, 0.75, 0)$ and $p_{e,2} = 1.5$, $p_{\parallel,2} = 0.75$ and $p_{\perp,2} = 4.5$. The results are shown in Fig. 2. All schemes increase the perpendicular temperature the most. The new scheme also increases the parallel temperature as $W_\parallel = 0.1$, while the other two schemes solving for the parallel pressure or parallel entropy equations do not deposit non-adiabatic heating into $p_\parallel$ and the parallel temperature $T_\parallel = p_\parallel/\rho$ remains constant. The three schemes produce different electron heatings: the new scheme deposits some of the non-adiabatic heating into the electrons because $W_e = 0.4$, the scheme solving for the electron entropy provides pure adiabatic heating for electrons, while the scheme solving for electron pressure heats the electrons in an unpredictable manner due to the non-conservative electron pressure equation.

Finally, we perform a test for an inclined shock. The initial conditions are $\rho_1 = 0.25$, $\mathbf{u}_1 = (-3.5, 0, 0)$, $\mathbf{B}_1 = (0.25, 0.25, 0)$, $p_{e,1} = p_{\parallel,1} = p_{\perp,1} = 0.25$ for $x > 0$ and $\rho_2 = 0.75$, $\mathbf{u}_2 = 0$, $\mathbf{B}_2 = (0.25, 0.75, 0)$, $p_{e,2} = p_{\parallel,2} = p_{\perp,2} = 2.5$ for $x < 0$. Fig. 3 shows the solution for three different schemes. For the new scheme $W_\parallel = 1/\sqrt{2} \approx 0.7$ from Eq. (34) to distribute the non-adiabatic heating. In this case both the perpendicular and parallel temperatures change across the shock at $x \approx 35$, as expected.

Fig. 4 shows the solutions using different numerical schemes (second order Rusanov versus first order HLLE schemes) with 500, 1000 and 1500 grid cells to demonstrate that the weak solution converges independent of the spatial discretization for the conservative methods, including the new algorithm, while it produces significantly different results for the non-conservative pressure equations.

4.2. 2D tests

We demonstrate the use of the new algorithm on a blast wave propagating into a magnetized low-pressure plasma. The equations are solved with the HLLE scheme [13] using the Koren limiter [14] on the primitive variables. The divergence of the magnetic field

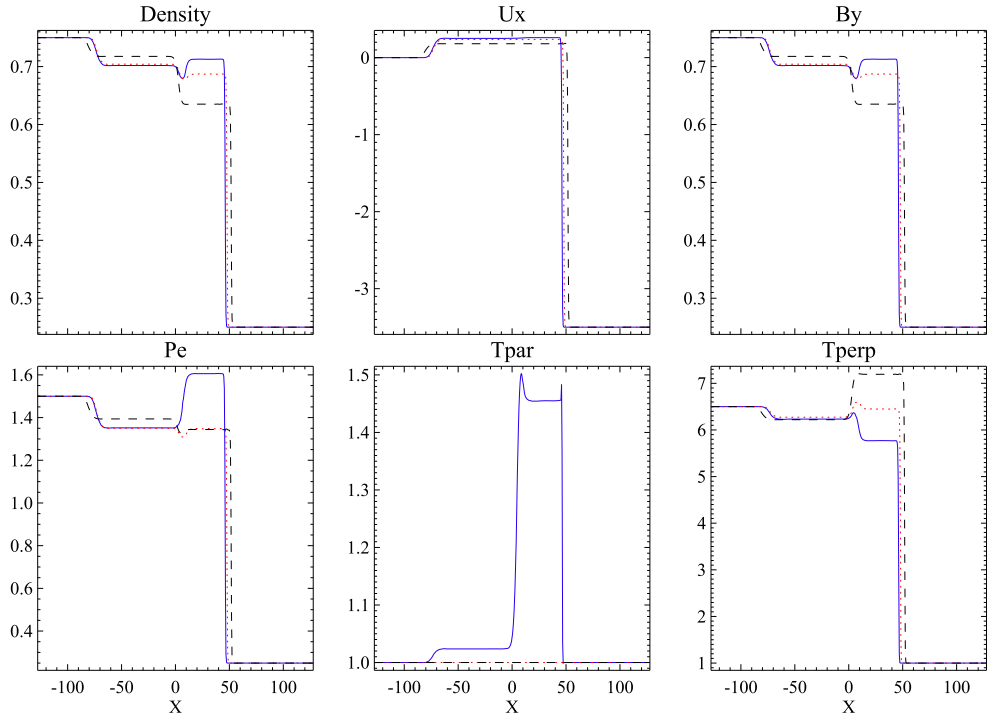

Fig. 2. Solution of the 1D perpendicular shock problem with the new algorithm solving for energy and entropy densities e, $s_{ie} = 0.4s_i - 0.6s_e$ and $s_\times = 0.9s_\parallel - 0.1s_\perp$ (solid blue line), conservative scheme solving for e, s_e and $s_\parallel$ (dotted red line) and energy conserving MHD scheme extended with non-conservative pressure equations solving for e, p_e and $p_\parallel$ (dashed black line).

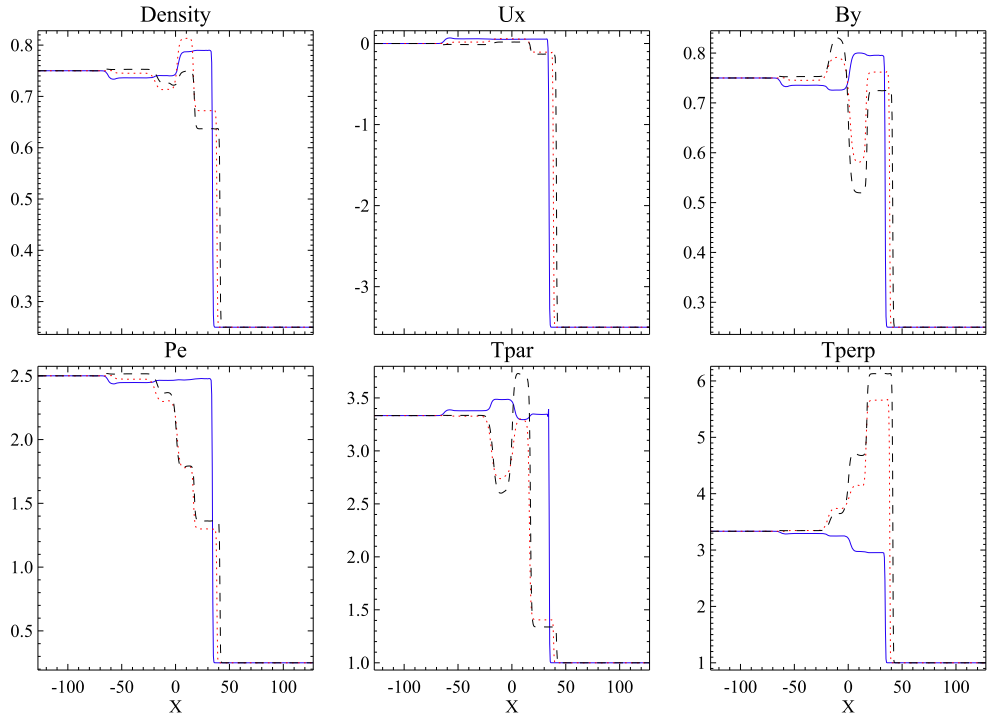

Fig. 3. Solution of the 1D inclined shock problem with the new algorithm solving for energy and entropy densities e, $s_{ie} = 0.4s_i - 0.6s_e$, $s_\times = 0.3s_\parallel - 0.7s_\perp$ (solid blue line), conservative scheme solving for e, $s_\parallel$ and s_e (dotted red line), and with energy conserving MHD scheme extended with non-conservative pressure equations solving for e, p_e and $p_\parallel$ (dashed black line).

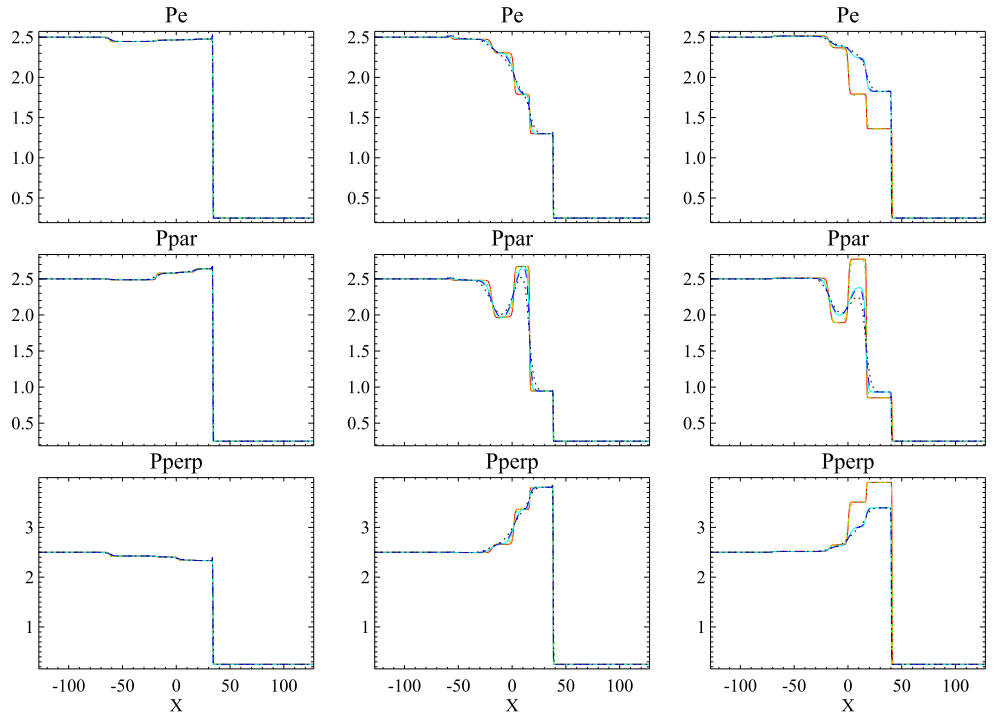

Fig. 4. Solution of the 1D inclined shock problem with the new algorithm solving for energy and entropy densities e, $s_{ie} = 0.4s_i - 0.6s_e$, $s_\times = 0.3s_\parallel - 0.7s_\perp$ (left column), conservative scheme solving for e, $s_\parallel$ and s_e (middle column), and with energy conserving MHD scheme extended with non-conservative pressure equations solving for e, p_e and $p_\parallel$ (right column) with second order Rusanov with 500 (dotted green line), 1000 (yellow dashed) and 1500 (solid red) grid cells and first order HLLE scheme with 500 (dotted black), 1000 (dashed dark blue) and 1500 (solid light blue) grid cells. Note that the lines mostly overlap for the conservative schemes (left and middle columns), but are very different for the non-conservative scheme (right column).

is controlled with the 8-wave scheme [7]. The computational domain is $0 < x, y < 1$ with double periodic boundaries resolved by a 200×200 uniform grid. The initial conditions are $\rho = 1$, $\mathbf{u} = 0$, and $\mathbf{B} = (1/\sqrt{2}, 1/\sqrt{2}, 0)$. The pressure is $p_1 = 0.1$ outside a circle of radius $r = 0.2$ centered around $x = y = 0.5$ and $p_2 = 10$ inside.

We perform two separate tests to study electron heating with isotropic ion pressure and anisotropic ion heating with no electron pressure, respectively, for the sake of clarity. In the first test we solve a separate electron pressure equation with isotropic ion pressure. Initially the pressure is distributed as $p_i = 0.9p$ and $p_e = 0.1p$. The adiabatic indexes are set to $\gamma_i = 5/3$ and $\gamma_e = 4/3$ and $W_e = 0.25$ for the new scheme. In the second test there is no electron pressure, but the ion pressure equation is anisotropic. Initially, however, we set $p_\parallel = p_\perp = p$ and take $W_\parallel$ from Eq. (34) allowing the full range from 0 to 1. In Eq. (34) the shock normal is estimated from the change in the velocity as $\mathbf{n} = \Delta\mathbf{u}/\Delta u$. Note that we do not explicitly detect the shock, but the non-adiabatic heating is only significant at the shock where the velocity change is parallel to the shock normal. The direction of the upstream magnetic field is taken from the initial and boundary condition: $\mathbf{B}_1 = (1/\sqrt{2}, 1/\sqrt{2}, 0)$. The simulations are stopped at $t = 0.2$.

Fig. 5 shows the ion and electron pressures obtained in the first test. The left column shows the results from the new algorithm depositing 25% of the non-adiabatic heating into the electrons. The middle column shows the results when solving for electron entropy with pure adiabatic heating. The ions are hotter and electrons are cooler in this case. Finally, the right panels show the solution using a non-conservative electron pressure equation. In this case the non-adiabatic electron heating depends on the numerical errors at the shock front. Interestingly, we had to switch to the minmod limiter for the conservative scheme with no electron heating (middle column) to avoid over and undershoots in the ion pressure. The other two simulations worked fine with the Koren limiter.

Fig. 6 shows the perpendicular and parallel pressures obtained in the second test. The left column shows the results from the new algorithm using Eq. (34) to distribute non-adiabatic heating between the parallel and perpendicular pressures. The middle column shows the results when solving for parallel entropy with pure adiabatic heating. The perpendicular pressure is enhanced and the parallel pressure is reduced in this case. Finally, the right panels show the solution using a non-conservative parallel pressure equation. In this case the non-adiabatic parallel heating depends on the numerical errors at the shock front.

Fig. 7 shows the solutions with the source terms enforcing the firehose and mirror stability conditions [2]. The solutions of the three schemes are more alike now, but still significantly different. This means that the stability conditions are insufficient to produce reliable weak solutions for MHD with anisotropic ion pressure. The new scheme, on the other hand, guarantees that the converged weak solution is not dependent on the discretization errors at the discontinuities.

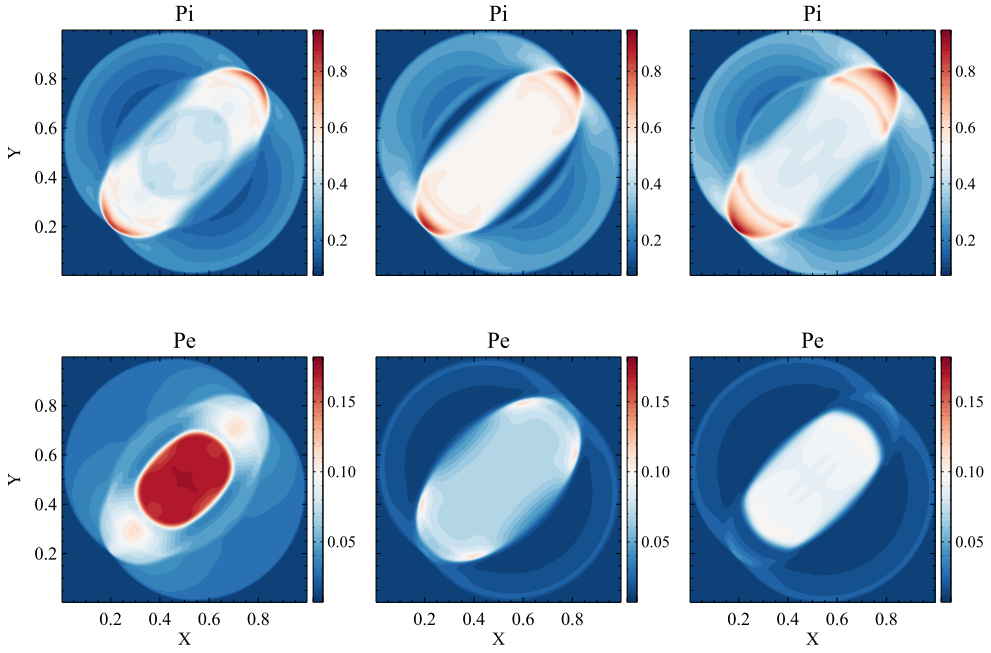

Fig. 5. Solution of the 2D blast wave problem with the new algorithm solving for energy and entropy densities e, $s_{ie} = 0.25 s_i - 0.75 s_e$ (left), with energy conserving MHD scheme extended with electron entropy equation solving for e and s_e (middle), and solving for e and non-conservative equation for p_e (right). The top panels show the ion pressure and the bottom panels the electron pressure.

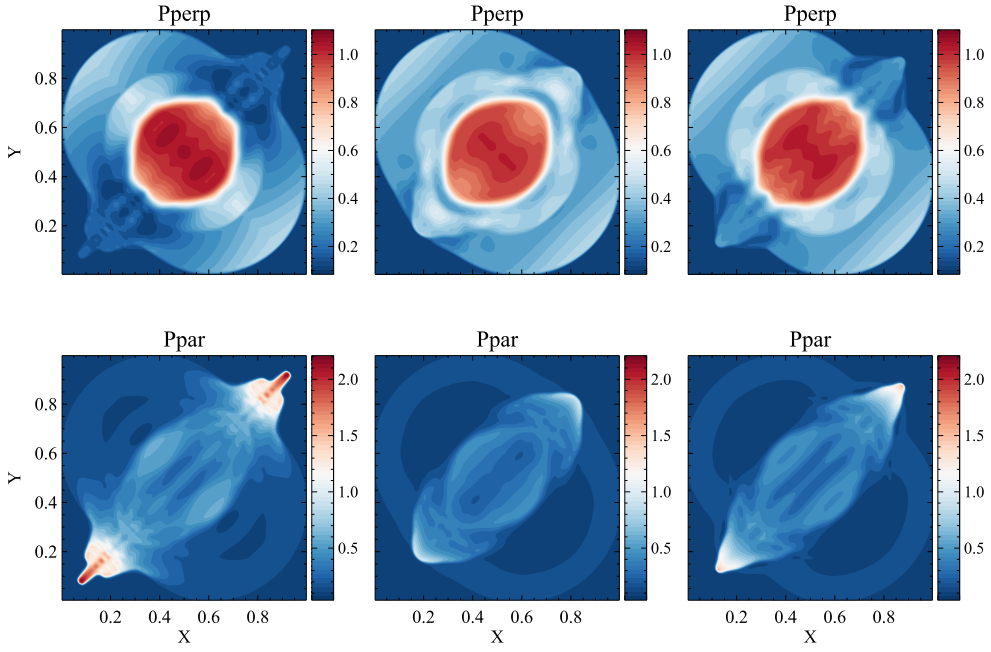

Fig. 6. Solution of the 2D blast wave problem with the new algorithm solving for energy and entropy densities e and $s_\times$ (left), with energy conserving MHD scheme extended with parallel entropy equation solving for e and $s_\parallel$ (middle), and solving for e and non-conservative equation for $p_\parallel$ (right). The top panels show the perpendicular pressure and the bottom panels the parallel pressure.

5. Conclusions

We have developed a new approach to obtain deterministic and physically well-motivated jump conditions across shocks in extended hydrodynamic and MHD simulations. We solve conservation equations for energy and linear combinations of entropy densities. The weights in the linear combination determine the fraction of non-adiabatic heating deposited into the various entropy densities. In particular, we can assign a fixed fraction of the non-adiabatic heating to electrons based on PIC simulation studies

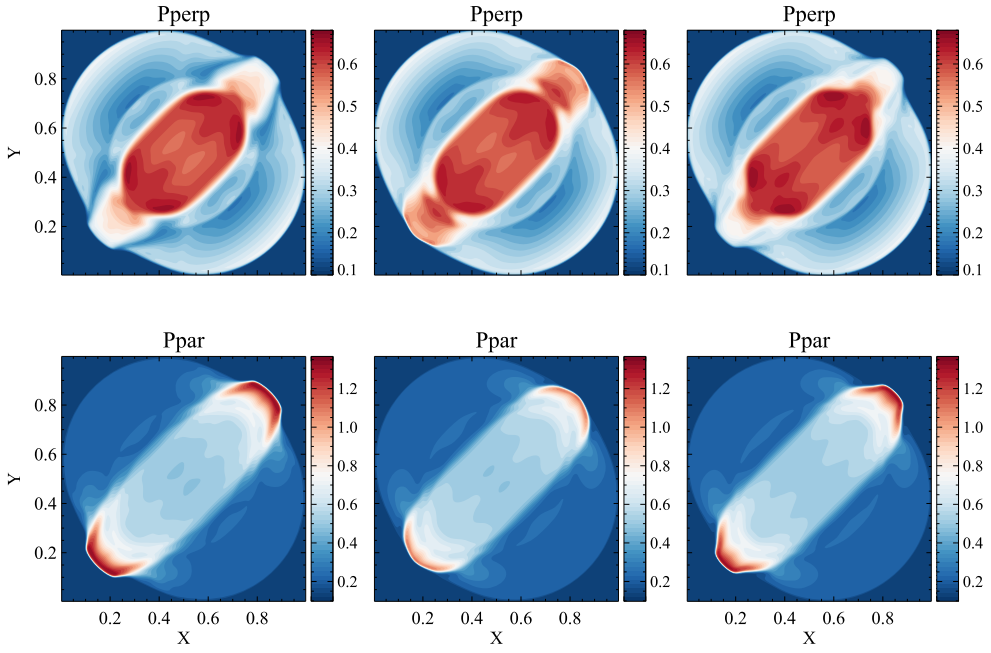

Fig. 7. Same as Fig. 6 but with the source terms enforcing the anisotropic stability conditions.

and satellite observations. For the anisotropic ion pressure, parallel and perpendicular shocks are expected to deposit most of the non-adiabatic heating into the parallel and perpendicular pressures, respectively. We have demonstrated the use of smoothly varying entropy weights (based on the upstream angle between the shock normal and the magnetic field) that transitions between the parallel and perpendicular shock cases.

The numerical tests suggest that the algorithm works as intended and provides solutions that are less dependent of the numerical scheme and closer to reality than the usual approaches using non-conservative pressure equations or conservative entropy equations with pure adiabatic heating. We note that we have not shown that the new scheme necessarily converges to entropy-based weak solutions. Proving such properties is left for future work.

The new scheme can also improve the numerical solution of reconnection at grid collapsed current sheets. While the reconnection rate itself depends on the numerical dissipation (see appendix of [15]), the new scheme can distribute the non-adiabatic Joule heating among the electron, parallel and perpendicular pressures in a way that is more consistent with kinetic simulations than a simple conservative scheme solving for e, s_e (and $s_\parallel$), which deposits most of the heat into the (perpendicular) ion thermal energy.

While in this paper we only discussed isotropic electron pressure, the ideas can be easily extended to the anisotropic electron pressure case. The parallel and perpendicular electron pressure equations have the same form as the corresponding ion pressure equations [16] as long as the electron and ion velocities are assumed to be the same, i.e. the Hall term is neglected. This means that the anisotropic electron entropy densities are completely analogous to the anisotropic ion entropy densities in Eqs. (9) and (10).

CRediT authorship contribution statement

Gábor Tóth: Writing – review & editing, Writing – original draft, Visualization, Software, Methodology, Investigation, Funding acquisition, Formal analysis, Data curation, Conceptualization. **Bart van der Holst:** Writing – review & editing, Methodology, Investigation, Formal analysis, Conceptualization.

Declaration of competing interest

The authors declare that they have no known competing financial interests or personal relationships that could have appeared to influence the work reported in this paper.

Data availability

Data will be made available on request.

Acknowledgement

The authors acknowledge support by the National Science Foundation grant PHY-2027555.

Appendix A. Entropy density functions and source terms

We show that if $\sigma = s/\rho$ is a specific entropy function per mass then an arbitrary differentiable function of σ can be used to define an alternative specific entropy function $\sigma_a = f(\sigma)$ and the corresponding alternative entropy density $s_a = \rho f(s/\rho)$. The conservation law for s_a can be expanded as

$$\frac{\partial(\rho\sigma_a)}{\partial t} + \nabla\cdot(\sigma_a\rho\mathbf{u}) = S_{s_a} \tag{A.1}$$

$$\sigma_a\frac{\partial\rho}{\partial t} + \rho f'(\sigma)\frac{\partial\sigma}{\partial t} + \sigma_a\nabla\cdot(\rho\mathbf{u}) + f'(\sigma)\rho\mathbf{u}\cdot\nabla\sigma = S_{s_a} \tag{A.2}$$

$$\sigma_a S_\rho + f'(\sigma)\left(\rho\frac{\partial\sigma}{\partial t} + \rho\mathbf{u}\cdot\nabla\sigma\right) = S_{s_a} \tag{A.3}$$

$$f(\sigma)S_\rho + f'(\sigma)(S_s - \sigma S_\rho) = S_{s_a} \tag{A.4}$$

where $f'(\sigma) = df(\sigma)/d\sigma$. The last equation defines S_{s_a} based on f, S_s and S_ρ.

Next we show that the conservation law for the entropy density function $s = p_e^{1/\gamma_e}$ results in the electron pressure equation (12). The conservation law for s is

$$\frac{\partial s}{\partial t} + \nabla\cdot(s\mathbf{u}) = S_s \tag{A.5}$$

$$\frac{1}{\gamma_e}p_e^{1/\gamma_e-1}\frac{\partial p_e}{\partial t} + \frac{1}{\gamma_e}p_e^{1/\gamma_e-1}\nabla p_e\cdot\mathbf{u} + p_e^{1/\gamma_e}\nabla\cdot\mathbf{u} = S_s \tag{A.6}$$

$$\frac{\partial p_e}{\partial t} + \nabla p_e\cdot\mathbf{u} + \gamma_e p_e\nabla\cdot\mathbf{u} = \gamma_e p_e^{1-1/\gamma_e}S_s \tag{A.7}$$

which is equivalent with Eq. (12) if $S_s = (\partial s/\partial p_e)S_{p_e} = (1/\gamma_e)p_e^{1/\gamma_e-1}S_{p_e}$. We can obtain the alternative electron entropy density s_e that is linear in the electron energy density e_e by applying the function $f(\sigma) = \sigma^{\gamma_e}$, so that $s_e = p_e/\rho^{\gamma_e-1}$. The source term for s_e can be obtained from Eq. (A.4):

$$S_{s_e} = f(\sigma)S_\rho + f'(\sigma)(S_s - \sigma S_\rho) \tag{A.8}$$

$$= \frac{p_e}{\rho_e^\gamma}S_\rho + \gamma_e\sigma^{\gamma_e-1}(S_s - \sigma S_\rho) \tag{A.9}$$

$$= (1-\gamma_e)\frac{p_e}{\rho_e^\gamma}S_\rho + \frac{1}{\rho^{\gamma_e-1}}S_{p_e} \tag{A.10}$$

$$= \frac{\partial s_e}{\partial\rho}S_\rho + \frac{\partial s_e}{\partial p_e}S_{p_e} \tag{A.11}$$

in agreement with Eq. (16). The derivation for the isotropic ion entropy density $s_i = p_i/\rho^{\gamma_i-1}$ is completely analogous and results in Eq. (17).

The conservation law for the perpendicular entropy density $s_\perp = p_\perp/B$ can be manipulated as follows:

$$\frac{\partial s_\perp}{\partial t} + \nabla\cdot(s_\perp\mathbf{u}) = S_{s_\perp} \tag{A.12}$$

$$\frac{1}{B}\frac{\partial p_\perp}{\partial t} - \frac{p_\perp\mathbf{B}}{B^3}\cdot\frac{\partial\mathbf{B}}{\partial t} + \frac{p_\perp}{B}\nabla\cdot\mathbf{u} + \frac{1}{B}\mathbf{u}\cdot\nabla p_\perp - \frac{p_\perp}{B^3}\mathbf{u}\cdot(\nabla\mathbf{B})\cdot\mathbf{B} = S_{s_\perp} \tag{A.13}$$

$$\frac{\partial p_\perp}{\partial t} + \frac{p_\perp\mathbf{B}}{B^2}\cdot[\nabla\cdot(\mathbf{uB}-\mathbf{Bu}) - \mathbf{S_B}] + p_\perp\nabla\cdot\mathbf{u} + \mathbf{u}\cdot\nabla p_\perp - \frac{p_\perp}{B^2}\mathbf{u}\cdot(\nabla\mathbf{B})\cdot\mathbf{B} = BS_{s_\perp} \tag{A.14}$$

$$\frac{\partial p_\perp}{\partial t} + \nabla\cdot(p_\perp\mathbf{u}) + p_\perp\nabla\cdot\mathbf{u} - p_\perp\mathbf{b}\cdot(\mathbf{b}\cdot\nabla\mathbf{u}) - \frac{p_\perp\mathbf{B}}{B^2}\cdot(\mathbf{S_B} + \mathbf{u}\nabla\cdot\mathbf{B}) = BS_{s_\perp} \tag{A.15}$$

where we introduced $\mathbf{b} = \mathbf{B}/B$ and $\mathbf{S'_B} = \mathbf{S_B} + \mathbf{u}\nabla\cdot\mathbf{B}$. We did not discard terms proportional to $\nabla\cdot\mathbf{B}$ for the sake of applications using the 8-wave scheme [7]. The last equation is the same as Eq. (15) except for the source terms, which have to satisfy

$$S_{s_\perp} = \frac{1}{B}S_{p_\perp} - \frac{p_\perp\mathbf{B}}{B^3}\cdot\mathbf{S'_B} = \frac{\partial s_\perp}{\partial p_\perp}S_{p_\perp} + \frac{\partial s_\perp}{\partial\mathbf{B}}\cdot\mathbf{S'_B} \tag{A.16}$$

The result agrees with Eq. (19).

Finally, the conservation law for the parallel entropy density $s_\parallel = p_\parallel B^2/\rho^2$ can be manipulated as

$$\frac{\partial s_\parallel}{\partial t} + \nabla\cdot(s_\parallel \mathbf{u}) = S_{s_\parallel} \tag{A.17}$$

$$\frac{B^2}{\rho^2}\frac{\partial p_\parallel}{\partial t} + \frac{2p_\parallel \mathbf{B}}{\rho^2}\cdot\frac{\partial \mathbf{B}}{\partial t} - \frac{2p_\parallel B^2}{\rho^3}\frac{\partial \rho}{\partial t} + \frac{p_\parallel B^2}{\rho^2}\nabla\cdot\mathbf{u} + \frac{B^2}{\rho^2}\mathbf{u}\cdot\nabla p_\parallel + \frac{2p_\parallel B}{\rho^2}\mathbf{u}\cdot\nabla B - \frac{2p_\parallel B^2}{\rho^3}\mathbf{u}\cdot\nabla\rho = S_{s_\parallel} \tag{A.18}$$

$$\frac{\partial p_\parallel}{\partial t} - \frac{2p_\parallel \mathbf{B}}{B^2}\cdot[\nabla\cdot(\mathbf{uB}-\mathbf{Bu}) - \mathbf{S_B}] - \frac{2p_\parallel}{\rho}S_\rho + 3p_\parallel\nabla\cdot\mathbf{u} + \mathbf{u}\cdot\nabla p_\parallel + \frac{2p_\parallel}{B^2}\mathbf{u}\cdot(\nabla\mathbf{B})\cdot\mathbf{B} = \frac{\rho^2}{B^2}S_{s_\parallel} \tag{A.19}$$

$$\frac{\partial p_\parallel}{\partial t} + \nabla\cdot(p_\parallel\mathbf{u}) + 2p_\parallel\mathbf{b}\cdot(\mathbf{b}\cdot\nabla)\mathbf{u} - \frac{2p_\parallel}{\rho}S_\rho + \frac{2p_\parallel\mathbf{B}}{B^2}\cdot\mathbf{S}'_\mathbf{B} = \frac{\rho^2}{B^2}S_{s_\parallel} \tag{A.20}$$

which is the same as Eq. (14) as long as

$$S_{s_\parallel} = \frac{B^2}{\rho^2}S_{p_\parallel} - \frac{2p_\parallel B^2}{\rho^3}S_\rho + \frac{2p_\parallel\mathbf{B}}{\rho^2}\cdot\mathbf{S}'_\mathbf{B} = \frac{\partial s_\perp}{\partial p_\perp}S_{p_\perp} + \frac{\partial s_\perp}{\partial\rho}S_\rho + \frac{\partial s_\perp}{\partial\mathbf{B}}\cdot\mathbf{S}'_\mathbf{B} \tag{A.21}$$

that is the same as Eq. (18).

In general, the source term for an entropy density s that is a function of the variables $\mathbf{U}$ is

$$S_s = \frac{\partial s}{\partial\mathbf{U}}\cdot\mathbf{S_U} \tag{A.22}$$

where $\mathbf{S_U}$ are the source terms for $\partial\mathbf{U}/\partial t$.

Appendix B. Alternative non-linear forms of the entropy densities

When forming a linear combination of multiple entropy densities, it seems useful to have the same physical dimensions for them. For the isotropic case $s_i = p_i/\rho^{\gamma_i-1}$ and $s_e = p_e/\rho^{\gamma_e-1}$ have the same dimensions when $\gamma_i = \gamma_e$. When the adiabatic indexes are different, one could switch to alternative definitions, such as

$$s'_i = \rho\ln\frac{C_i p_i}{\rho^{\gamma_i}} \tag{B.1}$$

$$s'_e = \rho\ln\frac{C_e p_e}{\rho^{\gamma_e}} \tag{B.2}$$

where C_i and C_e are constants with appropriate dimensions that make the arguments of the logarithm functions dimensionless. The disadvantage of these definitions is that it requires solving a nonlinear system of equations

$$W_e s'_i - W_i s'_e = s'_{i,e} \tag{B.3}$$

$$e_i + e_e = e_t \tag{B.4}$$

for the unknown energy densities e_i and e_t.

Similarly, an alternative form of the anisotropic entropy densities can be defined [17] as

$$s'_\parallel = \rho\frac{1}{3}\ln\frac{C_\parallel p_\parallel B^2}{\rho^3} \tag{B.5}$$

$$s'_\perp = \rho\frac{2}{3}\ln\frac{C_\perp p_\perp}{\rho B} \tag{B.6}$$

which have the same dimensions, moreover, they have the desired property that $s'_\parallel + s'_\perp = s'_i$ when $\gamma_i = 5/3$ and $p_\parallel = p_\perp$. On the other hand, the linear combination $s'_\times = W_\perp s'_\parallel - W_\parallel s'_\perp$ does not have any obvious physical meaning, and one needs to solve a non-linear system of equations for $e_\parallel$ and $e_\perp$.

References

[1] X. Meng, G. Tóth, I.V. Sokolov, T.I. Gombosi, Classical and semirelativistic magnetohydrodynamics with anisotropic ion pressure, J. Comput. Phys. 231 (2012) 3610–3622, https://doi.org/10.1016/j.jcp.2011.12.042.

[2] X. Meng, G. Tóth, M.W. Liemohn, T.I. Gombosi, A. Runov, Pressure anisotropy in global magnetospheric simulations: a magnetohydrodynamics model, J. Geophys. Res. 117 (2012) A08216, https://doi.org/10.1029/2012JA017791.
[3] X. Meng, B. van der Holst, G. Tóth, T.I. Gombosi, Alfven wave solar model (AWSoM): proton temperature anisotropy and solar wind acceleration, Mon. Not. R. Astron. Soc. 454 (2015) 3697, https://doi.org/10.1093/mnras/stv2249.
[4] C. Graziani, P. Tzeferacos, D. Lee, D.Q. Lamb, K. Weide, M. Fatenejad, J. Miller, The Biermann catastrophe in numerical magnetohydrodynamics, Astrophys. J. 801 (2015) 43, https://doi.org/10.1088/0004-637X/802/1/43.
[5] G.F. Chew, M.L. Goldberger, F.E. Low, The Boltzmann equation and the one-fluid hydromagnetic equations in the absence of particle collisions, Proc. R. Soc. Lond. Ser. A, Math. Phys. Sci. 236 (1956) 112–118.
[6] A. Tran, L. Sironi, Electron heating in perpendicular low-beta shocks, Astrophys. J. Lett. 900 (2020) L36, https://doi.org/10.3847/2041-8213/abb19c.
[7] K.G. Powell, An approximate Riemann solver for magnetohydrodynamics (that works in more than one dimension), Technical Report 94-24, Inst. for Comput. Appl. in Sci. and Eng., NASA Langley Space Flight Center, Hampton, Va, 1994.
[8] A. Johlander, Y.V. Khotyaintsev, A.P. Dimmock, D.B. Graham, A. Lalti, Electron heating scales in collisionless shocks measured by mms, Geophys. Res. Lett. 50 (2023), https://doi.org/10.1029/2022GL100400.
[9] K. Powell, P. Roe, T. Linde, T. Gombosi, D.L. De Zeeuw, A solution-adaptive upwind scheme for ideal magnetohydrodynamics, J. Comput. Phys. 154 (1999) 284–309, https://doi.org/10.1006/jcph.1999.6299.
[10] G. Tóth, B. van der Holst, I.V. Sokolov, D.L.D. Zeeuw, T.I. Gombosi, F. Fang, W.B. Manchester, X. Meng, D. Najib, K.G. Powell, Q.F. Stout, A. Glocer, Y.-J. Ma, M. Opher, Adaptive numerical algorithms in space weather modeling, J. Comput. Phys. 231 (2012) 870–903, https://doi.org/10.1016/j.jcp.2011.02.006.
[11] V. Rusanov, Calculation of interaction of non-steady schock waves with obstacles, J. Comp. Math. Phys. 1 (1961) 267.
[12] X. Meng, G. Tóth, A. Glocer, M.-C. Fok, T.I. Gombosi, Pressure anisotropy in global magnetospheric simulations: coupling with ring current models, J. Geophys. Res. 118 (2013) 5639, https://doi.org/10.1002/jgra.50539.
[13] B. Einfeldt, C.D. Munz, P.L. Roe, B. Sjögreen, On Godunov-type methods near low densities, J. Comput. Phys. 92 (1991) 273–295.
[14] B. Koren, A robust upwind discretisation method for advection, diffusion and source terms, in: C. Vreugdenhil, B. Koren (Eds.), Numerical Methods for Advection-Diffusion Problems, Vieweg, Braunschweig, 1993, p. 117.
[15] X. Wang, Y. Chen, G. Toth, Global magnetohydrodynamic magnetosphere simulation with an adaptively embedded particle-in-cell model, J. Geophys. Res. 127 (2022) e2021JA030091, https://doi.org/10.1029/2021JA030091.
[16] Z. Huang, G. Tóth, B. van der Holst, Y. Chen, T. Gombosi, A six-moment multi-fluid plasma model, J. Comput. Phys. 387 (2019) 134, https://doi.org/10.1016/j.jcp.2019.02.023.
[17] G.M. Webb, S.C. Anco, S.V. Meleshko, G.P. Zank, Action principles and conservation laws for Chew–Goldberger–Low anisotropic plasmas, 88 (2022) 835880402, https://doi.org/10.1017/S0022377822000642.